Design of methane hydrate inhibitor molecule using Density Functional Theory

S. Pal[1]*, T K Kundu[2]
[1]Department of Metallurgical and Materials Engineering, National Institute of Technology Rourkela, Rourkela –769008, India, [2]Department of Metallurgical and Materials Engineering, Indian Institute of Technology Kharagpur, Kharagpur –721302, India

*Corresponding Author: S. Pal, [1]Department of Metallurgical and Materials Engineering, National Institute of Technology Rourkela, Rourkela –769008, India.

Email: snehanshu.iitkgp.phd@gmail.com, Phone No. +91 -661 – 2462573, Fax No. +91 -661 – 2462550

[1] To whom any correspondence should be addressed.

Design of methane hydrate inhibitor molecule using Density Functional Theory

Abstract:

A strategy for designing methane hydrate inhibitor molecule has been established depending upon geometrical parameters, interaction energy, highest occupied molecular orbital (HOMO) - lowest unoccupied molecular orbital (LUMO) structures and energies, natural bond orbital (NBO) analysis, potential energy curve, Mullikan charge, IR intensity and red shift. One methane hydrate inhibitor molecule namely 2, 2'-oxydipropane-1, 3-diol has been designed based on the established design strategy. Theoretical study of effectiveness of the designed inhibitor molecule has been performed for methane hydrate pentagonal dodecahedron cage ($1CH_4@5^{12}$) using WB97XD/6-31++G(d,p). Calculated geometrical parameters, interaction energies and HOMO LUMO study indicate that reduction of the strength of hydrogen bonded network of $1CH_4@5^{12}$ cage is more by designed inhibitor 2,2'-oxydipropane-1,3-diol compared to conventional thermodynamic inhibitor (methanol) and consequently 2,2'-oxydipropane-1,3-diol can be more effective methane hydrate inhibitor than methanol.

Keywords: Density functional theory, Methane hydrates inhibitor, Natural bond orbital, and Red shift.

1. Introduction

Methane hydrate is non-stoichiometric clathrate compound stable at low temperature and high pressure. Methane hydrate is essentially one type of gas hydrate, formed by hydrogen bonded water cluster and contains methane gas molecules inside water cage. Guest molecule methane stabilizes the water cages of methane hydrate. Large deposit of methane hydrates are found in ocean sediments and underneath of permafrost region. These huge accumulations are considered to be significant future energy source [1]. Decomposition of methane hydrate can also cause global warming [2]. Methane hydrate has obtained strong attention because of its importance as a fuel and its environmental effects.

Gas hydrate has generally three types of conformations namely structure-I (consisting of two 5^{12} cages and six $5^{12}6^2$ cages), structure-II (consisting of sixteen 5^{12} cages and eight $5^{12}6^4$ cages) and structure-H (consisting of three 5^{12} cages, two $4^3 5^6 6^3$ cages, and one $5^{12}6^8$ cage) [3]. Oil and gas industry view methane hydrates as nuisance because its formation in pipeline disturbs flow assurance, reduces safety and increase operational and maintenance cost in petroleum industries [4, 5]. Thus restriction of gas hydrate formation is very important. Prevention of hydrate plug formation can be achieved by reducing the stability of gas hydrate phase using thermodynamic inhibitors [6, 7] and lingering of gas hydrate nucleation using kinetic inhibitors [4, 7] and anti-agglomerates [6]. Commonly used chemical inhibitors such as methanol, ethylene glycol and tri-ethylene glycol are thermodynamic inhibitors as their presence narrows down the gas hydrate stability region, so that gas hydrate cannot form in the operating pressure and temperature condition. Gas hydrate inhibitors can break hydrogen-bonded network of clathrate structure by forming itself comparatively stronger hydrogen bond with water molecules of clathrate hydrate. Detail understanding of hydrogen bond interaction is essential to identify potential gas hydrate inhibitor and design effective gas hydrate inhibitor and quantum chemical calculation can play a significant role in this regard..

Theoretical studies of different systems having hydrogen bond interactions like water complex [8], gas hydrate structure [9-19], tetrahydrofuran + water complex [20, 21] and methanol + water complex [22] have been carried out by researchers. To sum up, the literature of quantum chemical calculation based studies of hydrogen bond interaction for various complexes is huge [23-28]. However, in the area of theoretical study of the interaction of inhibitors with methane hydrate cage, only DFT studies of methanol + 5^{12} methane hydrate cage [29] and chitosan + 5^{12} cage [30] systems have been reported in literature so far. Variation on important structural, thermo-chemical, frontier orbital, NBO analysis and spectroscopic (IR intensity and red shift) parameters indicate methane hydrate inhibition characteristics of methanol [29] and chitosan [30] inhibitors. In presence of methanol average hydrogen bond distances of $1CH_4@5^{12}$ cage are found to be increased and consequently the strength of hydrogen bonded network of water molecules of this hydrate cage is decreased [29]. It is found that methanol and chitosan have strong donor acceptor interaction with water molecules of methane encapsulated pentagonal dodecahedron ($1CH_4@5^{12}$) cage and consequently weaken the $1CH_4@5^{12}$ cage structure [29, 30]. DFT based methodology for designing methane hydrate inhibitor molecule is essential as DFT is useful for material design considering the structure–property relationships and evaluating performance of newly designed materials. However, gas hydrate inhibitor design methodology based on DFT is not reported in literature till date. The objectives of this work are establishment of a comprehensive theoretical methodology for designing methane hydrate inhibitor molecule based on above structure-property correlation parameters and detail theoretical analysis to study the effect of designed methane hydrate inhibitor on the stability of $1CH_4@5^{12}$ hydrate cage.

2. Design methodology and simulation details

The effective utilization of DFT towards designing and studying of materials generally includes three steps [31] such as (i) formulation of the engineering problem to a computable atomistic model, (ii) computation of the required physicochemical properties, and (iii) validation of the simulation results with experimental data. Strategy for designing methane hydrate inhibitor molecules based on quantum chemical calculations includes construction of initial configuration of different complexes of hydrate cage and inhibitor molecule, geometry optimization and frequency calculation on optimized geometries of these complexes. Presence of polar functional group (e.g. -OH and $-NH_2$) and ether group in inhibitor molecules increases its water solubility property and biodegradability respectively. The shape of HOMO and LUMO of hydrogen bonded cluster helps to detect the covalent character of hydrogen bond interaction between hydrogen bonded components. Comparative study between potential energy curve of hydrogen bonded X-H bond and free X-H bond helps to determine the strength of hydrogen bond (X-H...Y). The extent of broadening of potential energy curve and position and nature of double minimum in a potential energy curve of hydrogen-bonded X-H bond can be applied to measure the strength of hydrogen bond. Hydrogen bond interaction between glycol and water (while glycol acts as a proton donor) is found to be strong as per respective potential energy curve of hydrogen bonded O-H bond [32, 33]. Mullikan charge difference between two hydrogen bonded atoms is useful to evaluate the strength of attraction between them. Second order perturbation energy is useful to evaluate the strength of donor acceptor interaction. IR intensity and red shift also helps to measure the strength of hydrogen bonded network of water molecules of methane hydrate cage with and without presence of inhibitor molecule. It is found from literature [29] that presence of methanol reduces the red shift value and IR intensity of O-H bond stretching of water molecules of $1CH_4@5^{12}$cage. All these quantum chemical evaluated structure-property

parameters quantify that an effective methane hydrate inhibitor should either have stronger hydrogen bond interaction with water molecules of methane hydrate cage or reduce hydrogen bond interaction between the water molecules of methane hydrate cage. In both ways methane hydrate inhibitor destabilizes the methane hydrate cage structure.

A theoretical methodology for methane hydrate inhibitor design has been proposed based on structural, thermo-chemical, frontier orbital, NBO analysis and spectroscopic (IR intensity and red shift) parameters. Some important practical attributes, like, water solubility, environment friendly character and non-combustibility have also been considered in formulating methane hydrate inhibitor designing methodology. This design methodology has been applied for designing new methane hydrate inhibitor molecule 2,2'-oxydipropane-1,3-diol. 2,2'-oxydipropane-1,3-diol molecule has one ether and four -OH groups. Multiple polar functional groups and ether group are incorporated in designed inhibitor molecule in order to have good water solubility and biodegradability. Detail theoretical study of hydrogen bond interaction of 2,2'-oxydipropane-1,3-diol molecule with water as well as with the $1CH_4@5^{12}$ cage has been presented in this paper to show the effective performance of the designed inhibitor molecule.

Geometry optimizations for 2,2'-oxydipropane-1,3-diol , complex of water and 2,2'-oxydipropane-1,3-diol molecule and another complex of $1CH_4@5^{12}$ cage and 2,2'-oxydipropane-1,3-diol molecule have been carried out using ωB97X-D/6-31++G(d,p) method. NBO analysis and frequency calculation for $1CH_4@5^{12}$cage + 2,2'-oxydipropane-1,3-diol have been performed using ωB97X-D/6-31++G(d,p) methods. ωB97X-D [34] functional considers additional dispersion energy term along with Kohn-Sham density functional theory [35,36] and also uses unscaled correction of dispersion term. Moreover, ωB97X-D functional includes the effect of dispersion on non-covalent interactions and describes effectively the non-covalent forces like hydrogen bonding and van der Waals

interactions. Therefore, ωB97X-D is good choice for density functional theory based investigation of gas hydrate system having van der Waals interactions.

Interaction energy (ΔE) for cluster formation has been determined using following equation,

$$\Delta E = E_{CLUSTER} - \sum E_{COMPONENTS} \quad (1)$$

Where, $E_{CLUSTER}$ and $E_{COMPONENTS}$ are optimized energy of cluster and individual components respectively. In case of NBO analysis, donor-acceptor interplay strength between filled orbital of the donor (ϕ_i) and the empty orbital of acceptor (ϕ_j) has been estimated by calculation of second order perturbation energy ($\Delta E_{ij}^{(2)}$) using following equation,

$$\Delta E_{ij}^{(2)} = 2\frac{<\phi_i \mid F \mid \phi_j>}{\varepsilon_i - \varepsilon_j} \quad (2)$$

where, ε_i and ε_j are NBO energies, F is Fock matrix element between the i and j NBO orbitals. Calculated vibrational frequency is scaled using 0.975 scaling factor [37].

3. Results and discussion

DFT based simulations of complexes of 2, 2'-oxydipropane-1,3-diol molecule with water and $1CH_4@5^{12}$ cage have been reported here to identify methane hydrate inhibition potential of 2, 2'-oxydipropane-1,3-diol. The optimized structures of 2,2'-oxydipropane-1,3-diol, complex of 2,2'-oxydipropane-1,3-diol molecule and 1 water complexes having water near to central ether group (configuration-1) and terminal hydroxyl group (configuration-2) of 2,2'-oxydipropane-1,3-diol using ωB97X-D/6-31++G(d,p) calculation are shown in **Fig. 1**. Here it is observed that inter-molecular hydrogen bond distances between water and 2,2'-oxydipropane-1,3-diol in both configurations are much less compared to intra-molecular

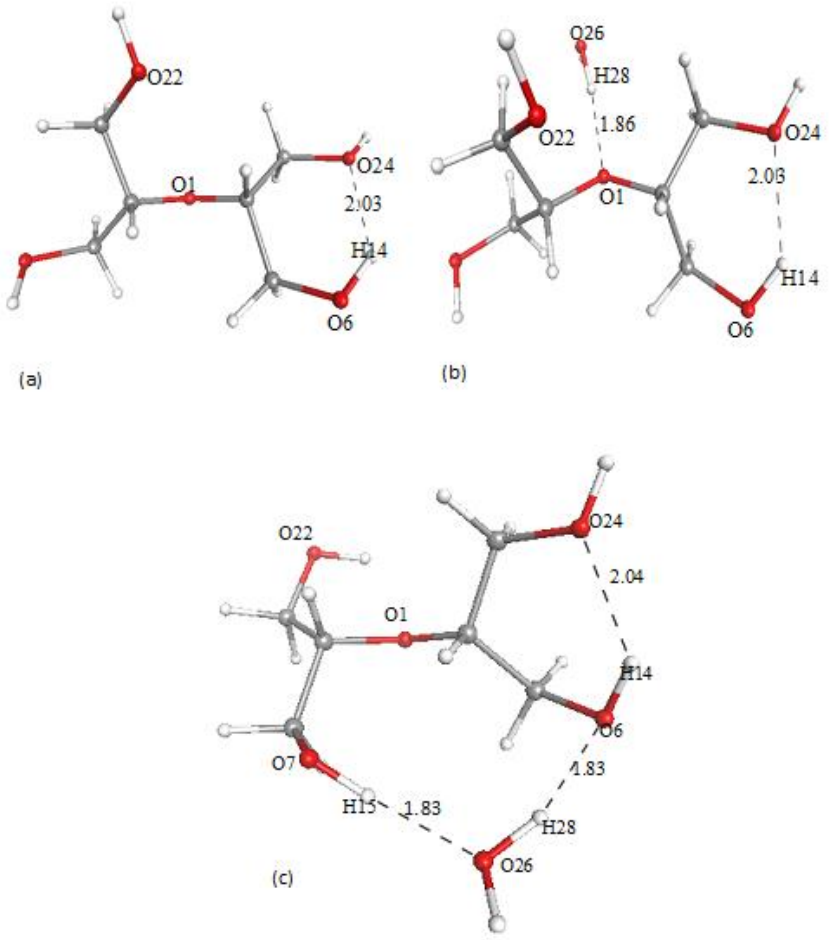

Fig. 1 Optimized structures of (a) 2,2'-oxydipropane-1,3-diol (b) 2,2'-oxydipropane-1,3-diol + 1 water configuration 1 (c) 2,2'-oxydipropane-1,3-diol + 1 water configuration 2 using ωB97X-D/6-31++G(d,p) (colour legend : red = oxygen , black = carbon and whitish grey = hydrogen and black dotted line is hydrogen bond and hydrogen bond distance in Å)

hydrogen bond distance ($d_{O...H}$) of 2,2'-oxydipropane-1,3-diol molecule. Accordingly, inter molecular hydrogen bonds between water and 2,2'-oxydipropane-1,3-diol are stronger than intra-molecular hydrogen bond of 2,2'-oxydipropane-1,3-diol molecule. The relative potential energy curves for intermolecular hydrogen bonded O-H (i.e. O7-H15 bond and O26-H28 bond) of 2,2'-oxydipropane-1,3-diol and 1 water complex configuration-2 has been calculated with respect to intermolecular hydrogen bonded O-H (i.e. O26-H28 bond) of

their complex configuration 1 and presented in **Fig. 2** . The broadening of those potential energy curves indicate strong intermolecular hydrogen bonds between water and 2,2'-oxydipropane-1,3-diol. The interaction energies for both configurations of complex consisting 2,2'-oxydipropane-1,3-diol molecule and one water are negative as evident in **Table 1**. All the above studies indicate strong hydrogen bond interaction between water molecule and 2,2'-oxydipropane-1,3-diol molecule.

Table 1 Calculated interaction energies (ΔE, kcal/mole) for 2, 2'-oxydipropane-1,3-diol + 1 water configurations and different cluster using ωB97X-D/6-31++G(d,p) method.

Complex	ΔE
2,2'-oxydipropane-1,3-diol + 1 water (configuration-1)	-8.169
2,2'-oxydipropane-1,3-diol + 1 water (configuration-2)	-16.45
$1CH_4@5^{12}$ cage	-208.23
Complex of $1CH_4@5^{12}$ cage and 2,2'-oxydipropane-1,3-diol	-222.69
Complex of Empty 5^{12} cage and2,2'-oxydipropane-1,3-diol	-215.31

Optimized structure of 5^{12} cage + 2,2'-oxydipropane-1,3-diol complex and $1CH_4@5^{12}$ cage + 2,2'-oxydipropane-1,3-diol complex using ωB97X-D/6-31++G(d,p) method are presented in **Fig. 3(a)** and **Fig. 3(b)** respectively. It is observed that two intermolecular hydrogen bonds between 2,2'-oxydipropane-1,3-diol and water molecules of both 5^{12} and $1CH_4@5^{12}$ cages are formed. The average and range of O-H bond length (d_{O-H}), hydrogen bond distance ($d_{O...H}$) and hydrogen bond angle ($A_{O\text{-}H...O}$) of 5^{12} cage and $1CH_4@5^{12}$ cage with and without presence of 2,2'-oxydipropane-1,3-diol are summarized in **Table 2**. The average hydrogen bond distance ($d_{O...H}$) for intermolecular hydrogen bonds among water molecules of $1CH_4@5^{12}$ cage is found to be increased in presence of 2,2'-oxydipropane-1,3-diol. It implies that 2,2'-oxydipropane-1,3-diol causes reduction in hydrogen bond strength. The range of

hydrogen bond distance and hydrogen bond angle are found to be expanded in presence of 2,2'-oxydipropane-1,3-diol for the both 5^{12} cage and $1CH_4@5^{12}$ cage. Standard deviation from average hydrogen bond distance and hydrogen bond angle become higher in presence of 2,2'-oxydipropane-1,3-diol for both 5^{12} cage and $1CH_4@5^{12}$ cage, as evident in **Table 2**. It can be inferred that some distortions of both 5^{12} cage and $1CH_4@5^{12}$ cage occurred in presence of 2,2'-oxydipropane-1,3-diol. It is also identified that interaction energy (ΔE) for hydrogen bonded cluster consisting of 5^{12} cage and 2,2'-oxydipropane-1,3-diol molecule is much less compared to 5^{12} cage. Similarly, interaction energy (ΔE) for another complex made of $1CH_4@5^{12}$ cage and 2,2'-oxydipropane-1,3-diol complexes is lower than that of $1CH_4@5^{12}$ cage. It is obvious that distortion of 5^{12} cage and $1CH_4@5^{12}$ cage in presence of 2, 2'-oxydipropane-1, 3-diol is taken place due to hydrogen bond interaction between 2,2'-oxydipropane-1,3-diol and water molecules of hydrate cages.

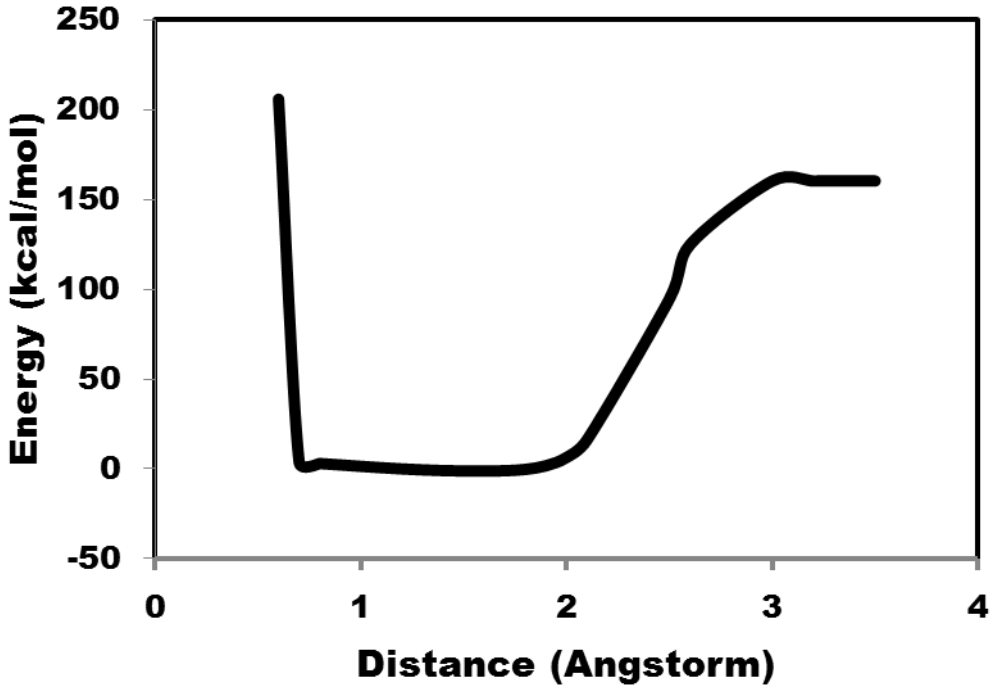

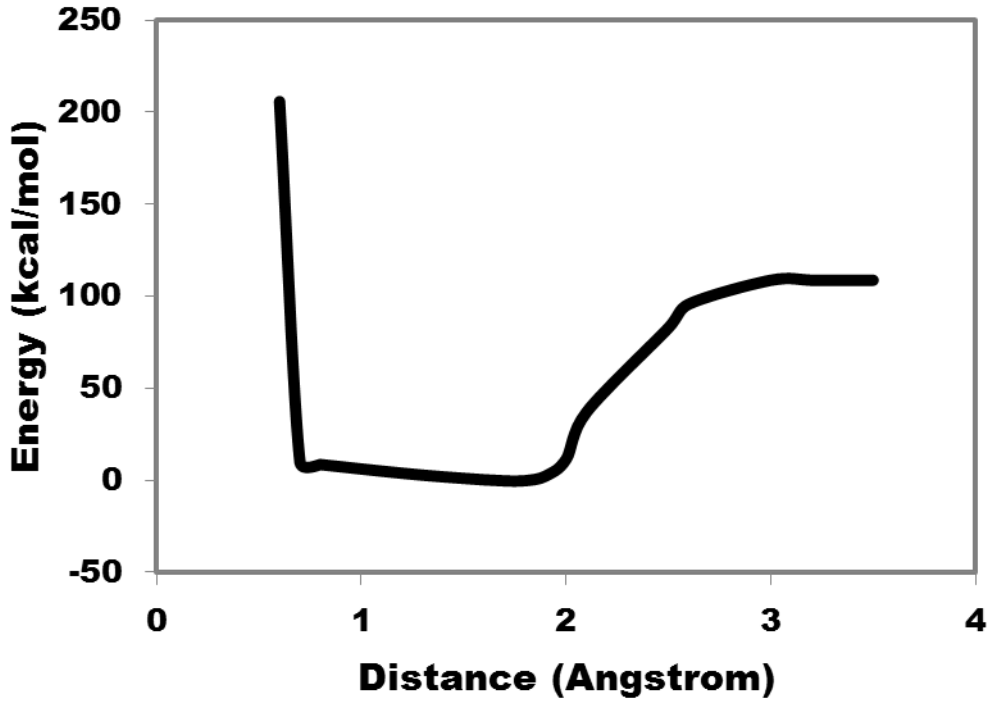

Fig.2 Relative potential energy curves for (a) hydrogen bonded O7-H15 bond (b) hydrogen bonded O26-H28 bond in 2,2'-oxydipropane-1,3-diol + 1 water (configuration-2) as in Fig. 1(c) with respect to hydrogen bonded O-H bond (O26-H28)) in 2,2'-oxydipropane-1,3-diol + 1 water (configuration-1) as in Fig. 1(b) .

Table 2 Calculated (at ωB97XD/6-31++G(d,p)) average O-H bond length (d_{O-H}, Å), hydrogen bond distance ($d_{O...H}$, Å) and hydrogen bond Angle ($A_{O-H...O}$, °) (Standard deviation is given in parenthesis)

Systems	d_{O-H}			$d_{O...H}$			$A_{O-H...O}$	
	Range	Avg.	Exp.	Range	Avg.	Exp.	Range	Avg.
$1CH_4@5^{12}$	0.963-0.996	0.976 (0.009)	0.861[338,15]	1.881-1.997	1.919 (0.037)	1.911[38,15]	169.9-180.0	175.6 (2.4)
Complex of $1CH_4@5^{12}$ and 2,2-oxy-dipropane-1,3-diol	0.960-0.991	0.971 (0.007)		1.874-2.002	1.930 (0.029)		142.3-178.0	170.3 (7.9)
Complex of Empty 5^{12} and 2,2'-oxy-dipropane-1,3-diol	0.960-0.991	0.971 (0.007)		1.935-2.002	1.930 (0.029)		142.3-77.86	170.3 (7.9)

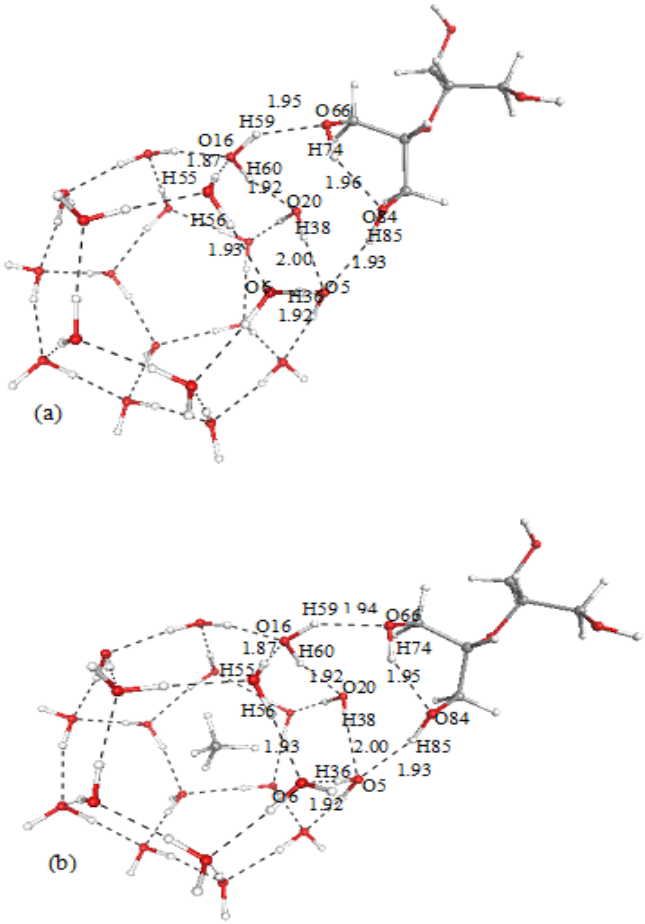

Fig. 3 Optimized structures of (a) 5^{12} cage + 2,2'-oxydipropane-1,3-diol (b) $1CH_4@5^{12}$ cage + 2,2'-oxydipropane-1,3-diol using ωB97X-D/6-31++G(d,p) (colour legend : red = oxygen , black = carbon and whitish grey = hydrogen and black dotted line is hydrogen bond and hydrogen bond distance in Å)

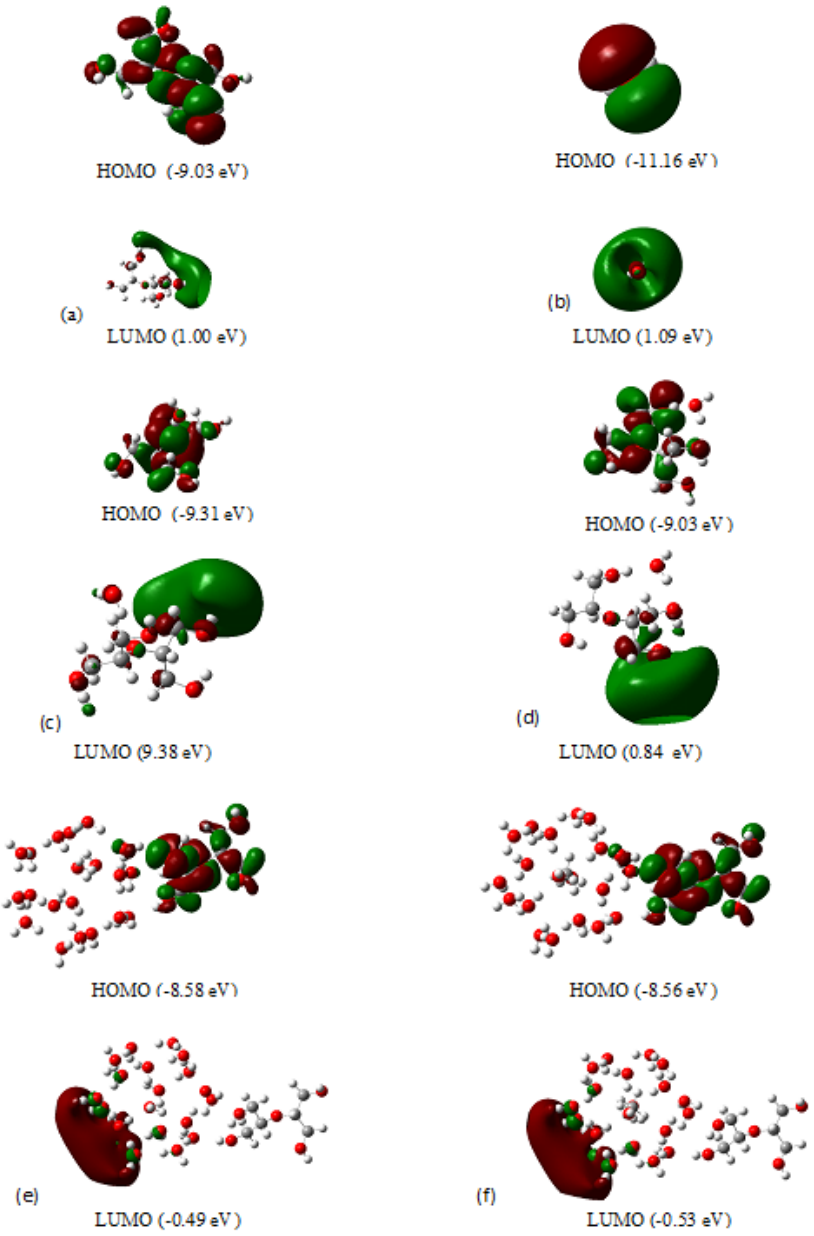

Fig. 4 HOMO-LUMO structures of (a) 2,2'-oxydipropane-1,3-diol (b) Water (c) 2, 2'-oxydipropane-1, 3-diol + 1 water configuration 1 (d) 2, 2'-oxydipropane-1, 3-diol + 1 water configuration 2 (e) 5^{12} cage + 2,2'-oxydipropane-1,3-diol (f) $1CH_4@5^{12}$ cage + 2,2'-oxydipropane-1,3-diol using ωB97X-D/6-31++G(d,p)

The calculated second order perturbation energies of some selective donor and acceptor interaction from NBO analysis using ωB97X-D/6-31++G(d,p) are shown in **Table 3**. The presence of donor–acceptor interactions are obvious from the calculated second order perturbation energy ($\Delta E_{ij}^{(2)}$) values of $1CH_4@5^{12}$ cage and $1CH_4@5^{12}$ cage + 2,2'-oxydipropane-1,3-diol configurations. It is observed from NBO investigation that the interaction between lone pair of oxygen atom and anti-bonding orbital of O-H of water molecules are usual donor acceptor nature in $1CH_4@5^{12}$ cage and complexes consisting of $1CH_4@5^{12}$ cage and 2,2'-oxydipropane -1,3-diol . The second order perturbation energy ($\Delta E_{ij}^{(2)}$) of donor–acceptor interaction between lone pair of hydrogen bond (O20...O16-H60) forming oxygen (O20) atom and anti bonding orbital of hydroxyl part (O16-H60) of $1CH_4@5^{12}$ cage is found to be reduced in presence of 2,2'-oxydipropane-1,3-diol. It shows that the presence of 2,2'-oxydipropane-1, 3-diol weakens the nearby intermolecular hydrogen bond (O20...O16-H60) between water molecules of $1CH_4@5^{12}$ cage. It is also observed that 2,2'-oxydipropane-1,3-diol forms intermolecular hydrogen bonds (e.g. O66... O16-H59) with the water molecules of $CH_4@5^{12}$ cage.

Table 3 Calculated second order perturbation energy ($\Delta E_{ij}^{(2)}$, kcal/mole) using ωB97X-D/6-31++G (d, p)

Donor NBO	**Acceptor NBO**	$\Delta E_{ij}^{(2)}$	
		$1CH_4@5^{12}$	Complex of $1CH_4@5^{12}$ and 2,2'-oxydipropane -1,3-diol
LP(2)O20	BD*(1)O16-H60	20.15	17.21
LP(2)O5	BD*(1)O20- H38	11.78	8.87
LP(2)O6	BD*(1)O5-H36	12.16	14.09
LP(1)O6	BD*(1)O17-H56	10.72	11.37
LP(2)O16	BD*(1)O17-H55	16.59	18.59
LP(2)O66	BD*(1)O16-H59		12.00
LP(2)O5	BD*(1)O84-H85		7.89
LP(2)O84	BD*(1)O66-H74		10.90

Simulated highest occupied molecular orbital (HOMO) and lowest unoccupied molecular orbital (LUMO) of 2,2'-oxydipropane-1,3-diol, 5^{12} cage, complex of 5^{12} cage and 2,2'-oxydipropane-1,3-diol complex, $1CH_4@5^{12}$ cage and complex of $1CH_4@5^{12}$ cage and 2,2'-oxydipropane-1,3-diol complex using ωB97X-D/6-31++G(d,p) methods have been presented in **Fig. 4**. The HOMO of 5^{12} cage + 2,2'-oxydipropane-1,3-diol complex originates essentially from the HOMO of 2,2'-oxydipropane-1,3-diol with negligible contribution of anti bonding orbital of 5^{12} cage, but the LUMO of the same complex arises largely from the LUMO of 5^{12} cage. Similarly, HOMO of $1CH_4@5^{12}$ cage + 2, 2'-oxydipropane-1,3-diol complex originates essentially from the HOMO of 2,2'-oxydipropane-1,3-diol with negligible contribution of anti bonding orbital of $1CH_4@5^{12}$ cage, but the LUMO of the same complex arises largely from the LUMO of $1CH_4@5^{12}$ cage. It can be inferred that intermolecular hydrogen bonds between 2,2'-oxydipropane-1,3-diol and 5^{12}cage or $1CH_4@5^{12}$ cage has strong covalent character.

Calculated vibrational frequencies of O-H stretching in water, 2,2'-oxydipropane-1,3-diol, water dimer, complex of water and 2,2'-oxydipropane-1,3-diol cluster are summarized along with some experimental values in **Table 4**. It is observed that red shifts of O-H vibrational frequencies for all the clusters are taken place due to the formation of hydrogen bonded network. The red shifts of vibrational frequencies are the consequence of hyper-conjugation interaction for conventional hydrogen bond formation.

Table 4 Calculated vibrational frequency (cm^{-1}), red shift (cm^{-1}), and IR intensity ($km\text{-}mol^{-1}$) of O-H bond stretching using ωB97X-D/6-31++G (d,p)

Systems	O–H stretching of water			O–H stretching of 2,2'- oxydipropane -1,3-diol		
	Scaled freq.	Red shift	IR Intensity	Scaled freq.	Red shift	IR Intensity
Water	3802		8.2			
Water dimer	3587	215	344.4			
2,2'-oxydipropane-1,3-diol				3751		96.07
Complex of 2,2'-oxydipropane-1,3-diol and 1 water (configuration- 1)	3503	299	478.17	3667	84	118.60
Complex of 2,2'-oxydipropane-1,3-diol and 1 water (configuration-2)	3535	267	477.27	3601	150	545.54

Red shift (cm^{-1}) and IR intensity ($km\text{-}mol^{-1}$) of O-H bond stretching for water molecules of $1CH_4@5^{12}$ cage in presence of 2,2'-oxydipropane-1,3-diol is lesser compared to that of $1CH_4@5^{12}$ cage in presence of methanol (refer supplementary information). Therefore, it can be inferred that the reduction of the strength of hydrogen bonded network of $1CH_4@5^{12}$ cage is more by designed inhibitor 2,2'-oxydipropane-1,3-diol compared to conventional thermodynamic inhibitor (methanol). Additionally, designed inhibitor 2, 2'-oxydipropane-1,3-diol has ether group and consequently it is also environment friendly inhibitor.

4. Conclusion

Methane hydrate inhibitor design strategy has been formulated based on structure property correlation attributes like geometrical parameters, interaction energy, HOMO-LUMO, NBO analysis, potential energy curve, Mullikan charge, IR intensity and red shift. One inhibitor molecule 2,2'-oxydipropane-1,3-diol has been proposed based on this design strategy. First principle based calculation have been performed to explain scientifically the role of designed molecule 2,2'-oxydipropane-1,3-diol as inhibitor of methane hydrate. The presence of designed inhibitor 2,2'-oxydipropane-1,3-diol molecule decrease the hydrogen bond strength and consequently the stability of $1CH_4@5^{12}$ cage, as revealed by studies of calculated interaction energies and geometrical parameters, NBO analysis, red shift, IR intensity. It is

observed that designed inhibitor 2,2'-oxydipropane-1,3-diol weakens the strength of hydrogen bonded network of $1CH_4@5^{12}$ cage more effectively compared to conventional thermodynamic inhibitor methanol. In addition to that, 2, 2'-oxydipropane-1,3-diol is environment friendly as it has ether group. This work clearly demonstrates the effective application of proposed design methodology for designing better methane hydrate inhibitor molecule. The study can be extended to develop design strategy for proposing better promoter and inhibitor molecule of all types of gas hydrates.

Acknowledgement

This work is financially supported by Ministry of Earth Science, Govt. of India (Project No. MoES/16/48/09-RDEAS (MRDM5)).

Conflict of interest

Authors declare no conflict of interest.

References

1. T. S. Collet, AAPG Bulletin 86, 1971 (2002)
2. P. Englezos, J. D. Lee, Korean J. Chem. Eng. 22, 671 (2005)
3. E. D. Sloan Jr., Nature 426, 353 (2003).
4. E. G. Hammerschmidt, Ind. and Eng. Chem. 26, 851 (1934).
5. J. K. Fink, Petroleum Engineer's Guide to Oil Field Chemicals and Fluids, 1st edn. (Elsevier, Oxford, 2012)
6. L. C. Jacobson, W. Hujo, V. Molinero, J. Am. Chem. Soc. 132, 11806 (2010).
7. J. Vatamanu, P. G. Kusalik, Phys. Chem. Chem.Phys. 12, 15065 (2010).
8. D. Peeters, J. Mol. Liq. 67, 49 (1995).
9. S. Pal, T. K. Kundu, J. Petro. Eng. and Tech. 2, 22 (2012)
10. H. K. Srivastava, G. N. Sastry, J. Phy. Chem. A 115, 7633 (2011).

11. T. M. Inerbaev, V. R. Belosludov, M. Sluiter , Y. Kawazoe, J. Kudoh, J. Inclusion Phen. Macrocyclic Chem. 48, 55 (2004).
12. F. Lebsir, A. Bouyacoub, D. Bormann, A. Krallafa, J. Mol. Struc. : Theochem 864, 42 (2008).
13. G. R. Román-Pérez, M. Moaied, J. M. Soler, F. Yndurain Phy. Rev. Lett. 105, 1459011 (2010).
14. P. K. Chattaraj, S. Bandaru, S. Mondal, J. Phy. Chem. A 115, 187 (2011).
15. Q. Li, B. Kolb, G. Román-Pérez, J. M. Soler, F. Yndurain, L. Kong, D. C. Langreth, T. Thonhauser, Phy. Rev. B 84, 1 (2011).
16. A. Lenz, L. Ojamäe, J. of Phy. Chem. A 115, 6169 (2011).
17. R. V. Belosludov, H. Mizuseki, M. Souissi, Y. Kawazoe, J. Kudoh, O. S. Subbotin, T. P. Adamova, V. R. Belosludov J. .Struc. Chem. 53, 619 (2012).
18. S. Pal, T. K. Kundu, J. Petro. Eng. and Tech. 2, 40 (2012).
19. S. Pal, T. K. Kundu, J. Petro. Eng. and Tech. 2, 1 (2012).
20. P. K. Sahu, A. Chaudhari, S. Lee, Chem. Phys. Lett. 386, 351 (2004).
21. P. K. Sahu and S. Lee The J. Chem. Phys. 123, 044308 (2005).
22. A. Mandal, M Prakash, R M Kumar, R Parthasarathi,V Subramanian, J. Phys. Chem. A 114, 2250 (2010).
23. J. E. D. Bene, Struct. Chem. 1, 19 (1989).
24. I. Alkorta, F. Blanco, P. M. Deyá, J. Elguero, C. Estarellas, A. Frontera, D. Quiñonero, Theor. Chem. Acc. 126 1 (2010).
25. I. Mata, E. Molins, I. Alkorta, E. Espinosa, J. Phys. Chem. A 111, 6425 (2007).
26. J. B. Levy, N. H. Martin, I. Hargittai, M. Hargittai J. Phys. Chem. A 102, 274 (1998).
27. O. V. Shishkin, I. S. Konovalova, L. Gorb, J. Leszczynski, Struct. Chem. 20, 37 (2009).

28. V. Horváth, A. Kovács and I. Hargittai J. Phys. Chem. A 107, 1197 (2003).

29. S. Pal, T. K. Kundu J. Chem. Sci. 125 379 (2013).

30. S. Pal, T. K. Kundu, Chem. Sci. Trans. 2, 447 (2013).

31. J. Hafner, C. Wolverton, G. Ceder, MRS Bulletin 31, 659 (2006).

32. S. Pal, T. K. Kundu, ISRN Phy. Chem. (2013) Article ID 753139.

33. S. Pal, T. K. Kundu, ISRN Phy. Chem. (2012), Article ID 570394.

34. J. Chai, M. Head-Gordon, Phys. Chem. Chem. Phys. 10, 6615 (2008).

35. P. Hoherberg, W. Kohn, Phys. Rev. 136, B864 (1964).

36. W. Kohn, L. J. Sham, Phys. Rev. 140, A1133 (1965).

37. I. M. Alecu, J. Zheng, Y. Zhao and G. Truhlar, J. Chem. Theo. and Comp. 6, 2872 (2010).

38. M. T. Kirchner, R. Boese, W. E. Billups, L. R. Norman, J. Am. Chem. Soc. 126, 9407 (2004).